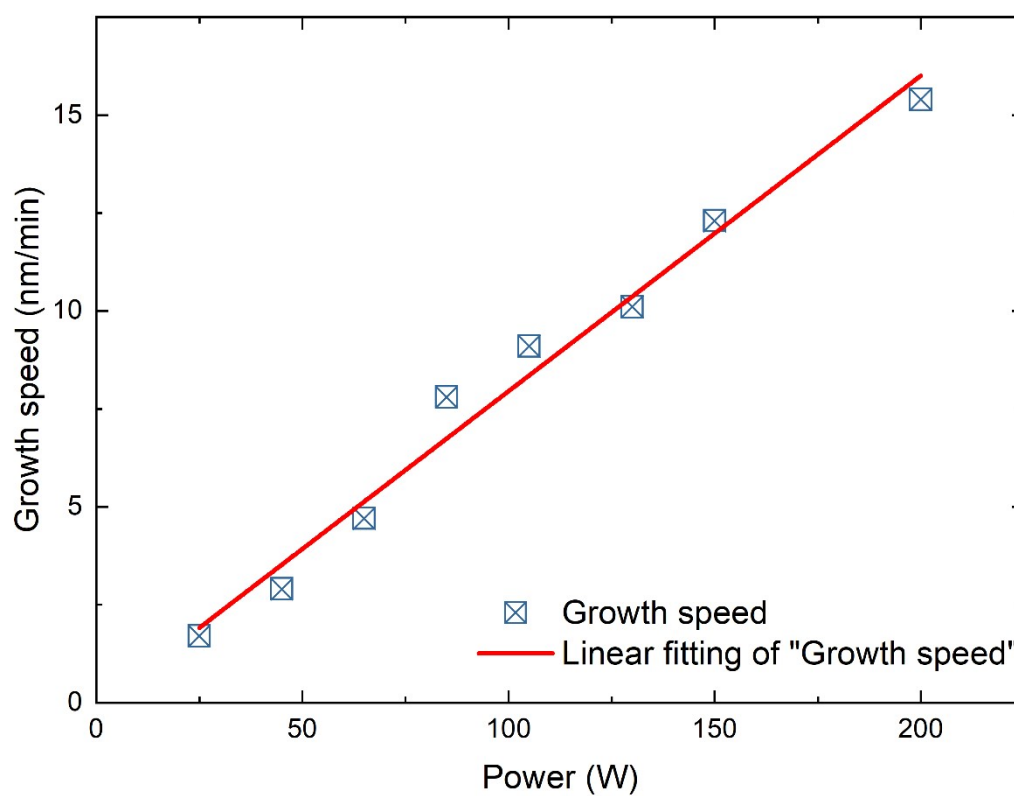


## Supporting Information

### Temperature and Environmental Stable Titanium Carbide as Electron-Selective Heterocontact for Crystalline Silicon Solar Cells

*Yang Ding, Zhiping Huang, Deyuan Wei\*, Jingwei Chen, Biao Sun, Chong Di, Jianming Wang, Kangping Zhang, Ying Xu\*, Guangsheng Fu\**



**Figure S1.** Growth speed of 200 W 2.0 Pa RF-sputtered  $\text{TiC}_x$  film.

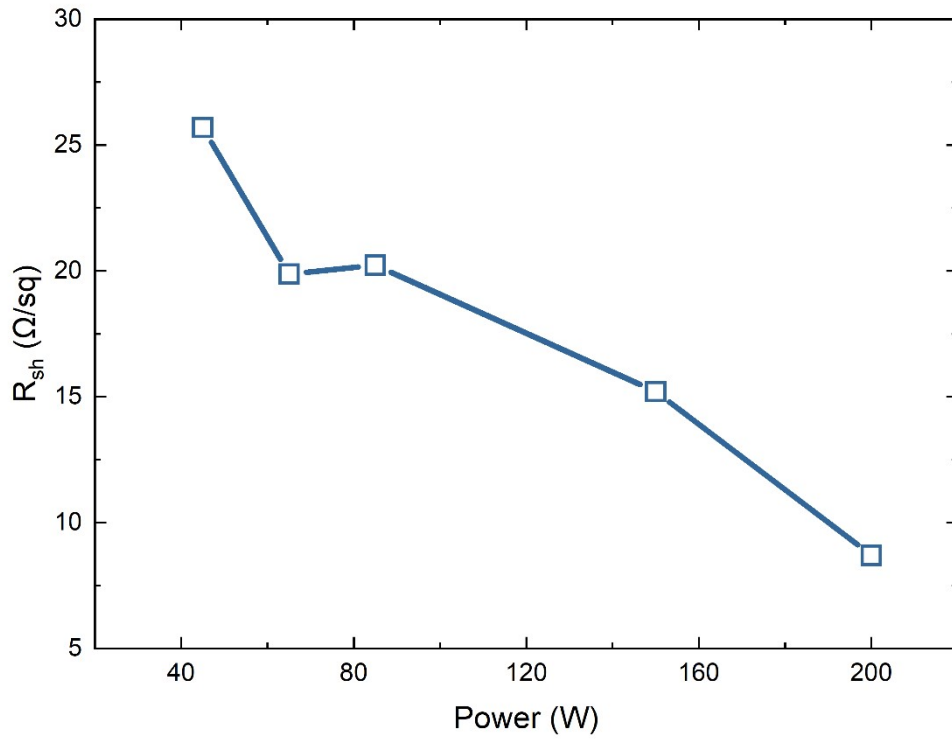


**Figure S2.** Square resistance of 300 nm  $TiC_x$  films at different sputtering powers with working pressure of 2.0 Pa.

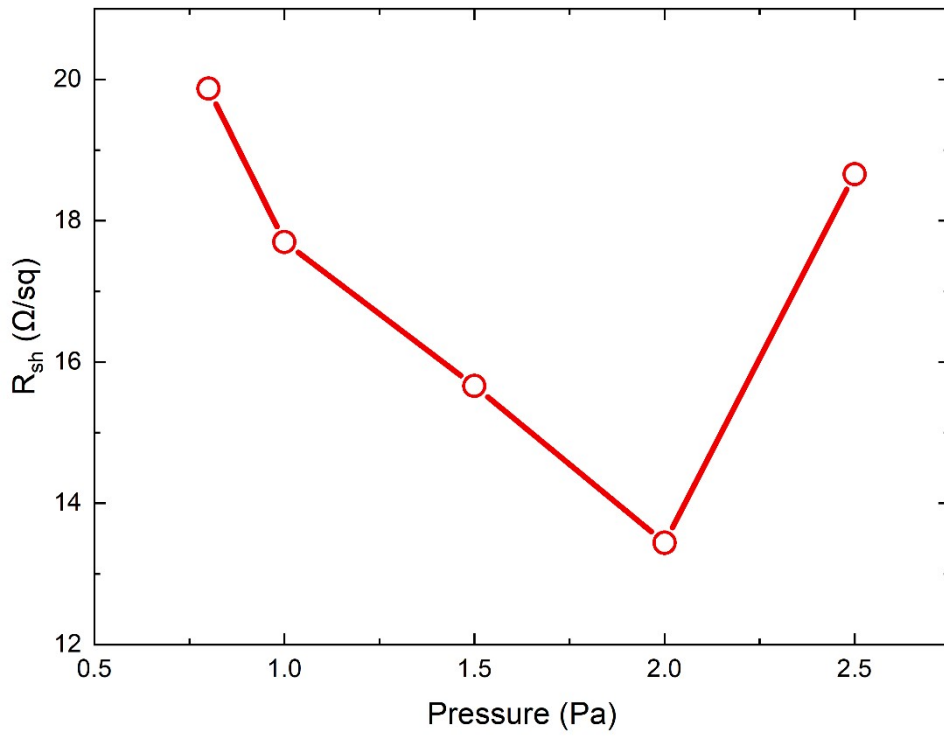


**Figure S3.** Square resistance of 300 nm  $TiC_x$  films at different working pressures with sputtering power of 200 W.

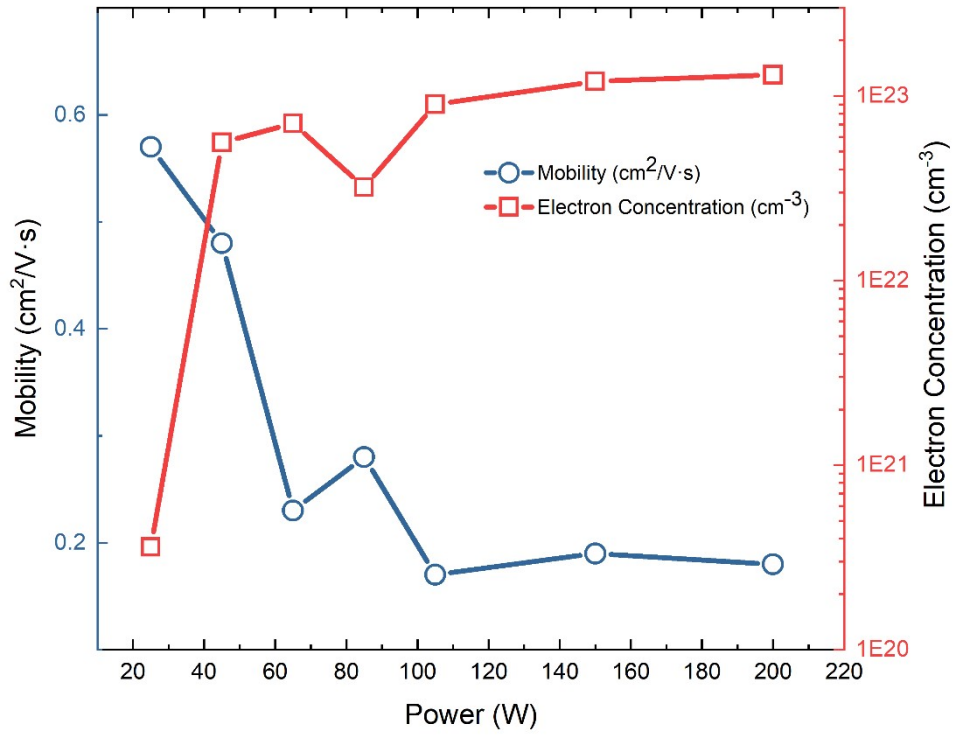


**Figure S4.** Electron concentration and mobility at different sputtering powers.

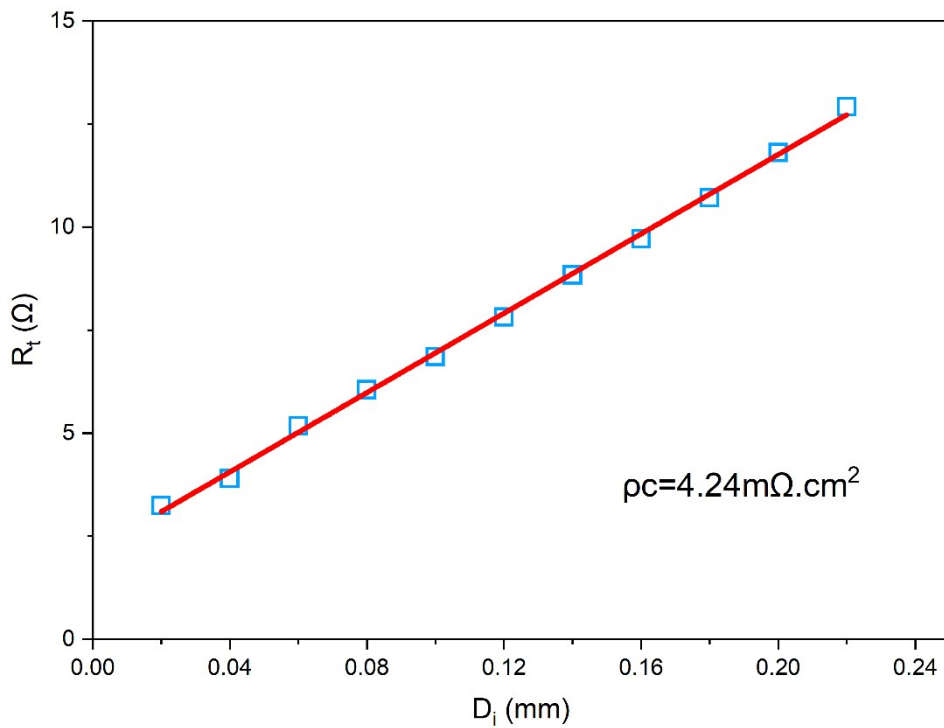


**Figure S5.** Linear fit to  $R_t$  to calculate contact resistivity.

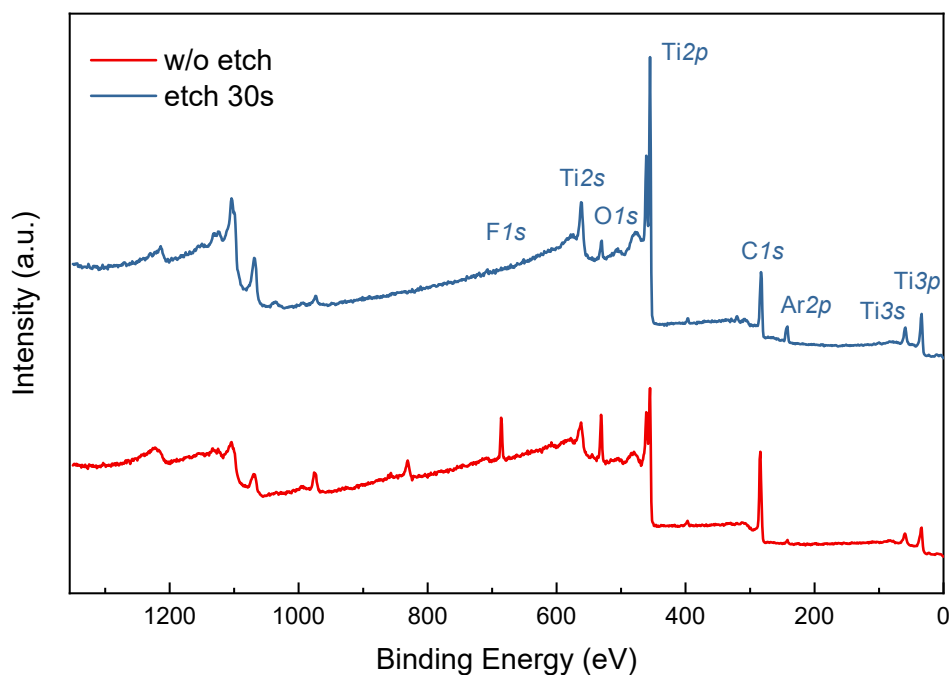


**Figure S6.** XPS survey of 200 W 2.0 Pa sputtered  $\text{TiC}_x$  film before and after surface etching.

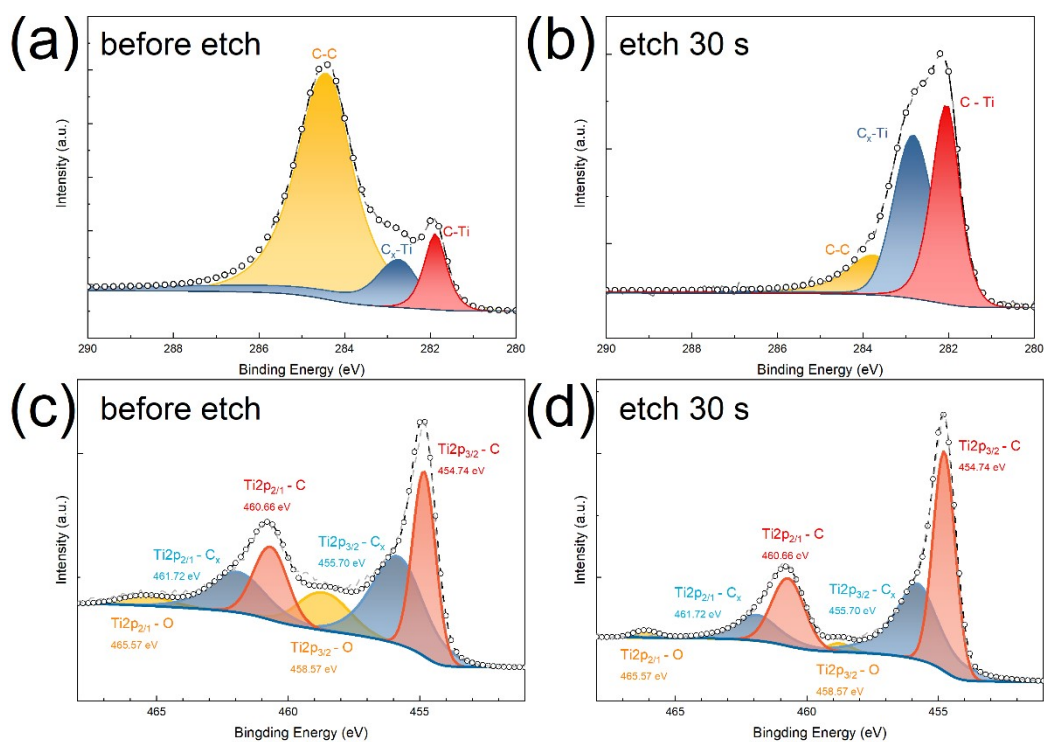


**Figure S7.** **a)** and **b)** XPS core-level spectra of  $\text{C}1s$  for the  $\text{TiC}_x$  films before and after surface etching, **c)** and **d)** XPS core-level spectra of  $\text{Ti}2p$  for the  $\text{TiC}_x$  films before and after surface etching.

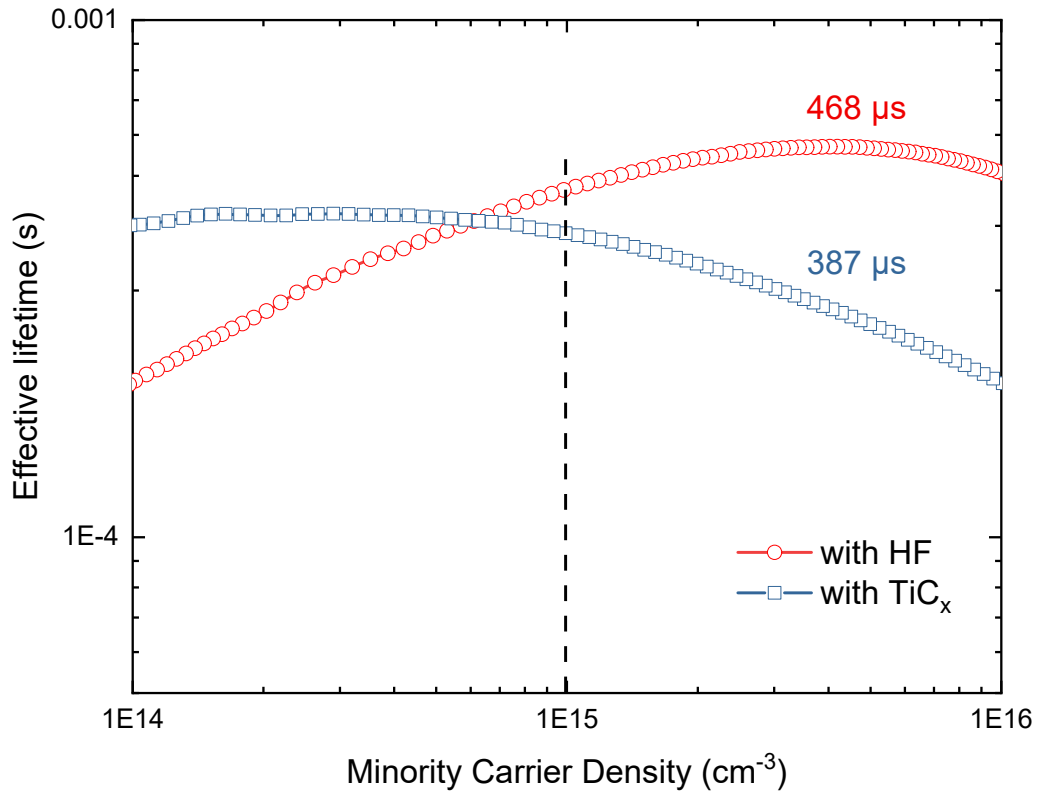


**Figure S8.** The effective minority carrier lifetimes of n-Si substrate (FZ, 3  $\Omega\text{cm}$ ) passivated by 5 nm  $\text{TiC}_x$  thin film or HF treatment.

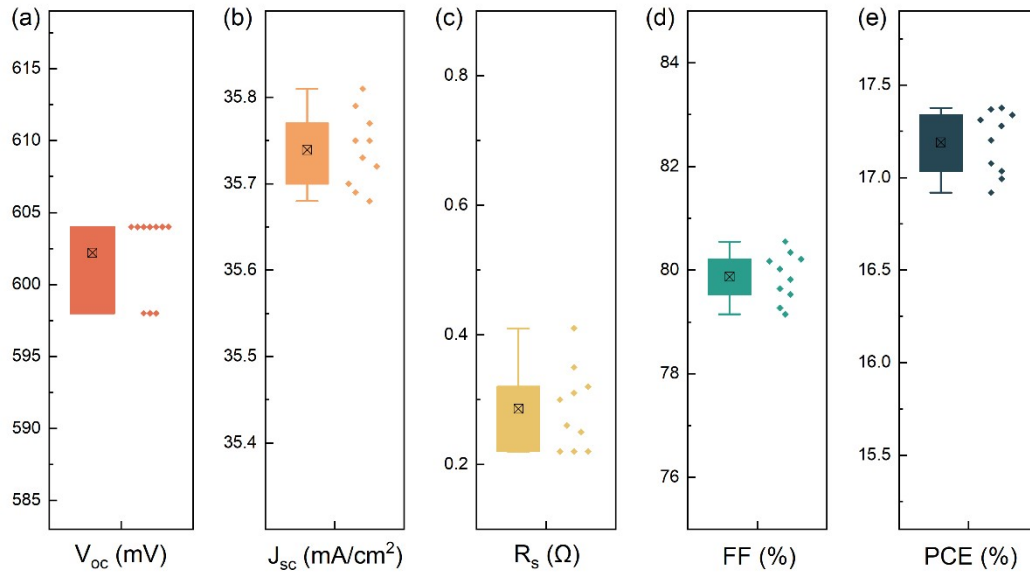


**Figure S9.** Reproducibility of the device with  $\text{TiC}_x$  ETL.

**Table S1.** Thermal stability Key parameters of representative silicon solar cells, device configurations and best power conversion efficiencies (PCE).

Materials	Contact structure	Thickness	Withstand temperature (°C)	PCE (%)	Reference
TiO <sub>x</sub>	n-Si/ SiO <sub>2</sub> / TiO <sub>x</sub> / Al/ Ag	3.5	300	20.5	[1]
TiO <sub>x</sub> /LiF/Al	n-Si/ a-Si:H(i)/ TiO <sub>x</sub> / LiF/ Al	1.5	300 <sup>b)</sup>	20.7	[2]
TiO <sub>x</sub> /LiF/Yb	n-Si/ a-Si:H(i)/ TiO <sub>x</sub> / LiF/ Yb/ Ag	1.0	175 <sup>b)</sup>	19.2	[3]
MgO <sub>x</sub>	n-Si/ MgO <sub>x</sub> / Al	1.0	400	20.0	[4]
Sc	n-Si/ SiO <sub>2</sub> / Sc/ Al	14.0	700	14.2	[5]
TiO <sub>x</sub>	n-Si/ SiO <sub>2</sub> / TiO <sub>x</sub> / Al	4.5	300	21.6	[6]
TiO <sub>x</sub>	n-Si/ TiO <sub>x</sub> / Al <sup>d)</sup>	1.5	400	23.1	[7]
TiO <sub>x</sub> /Yb	n-Si/ a-Si:H(i)/ TiO <sub>x</sub> / Yb/ Ag	1.0	300 <sup>b)</sup>	17.6	[8]
YbSi <sub>x</sub>	n-Si/ a-Si:H(i)/ YbSi <sub>x</sub> / Ag	2.1	300 <sup>b)</sup>	17.0	[9]
AMC or AEMC <sup>a)</sup>	n-Si/ AMC or AEMC/ Al	1.0	350 <sup>b)</sup>	19.4	[10]
MAcac <sup>c)</sup>	n-Si/ a-Si:H(i)/ MAcac/ Al	1.0	350 <sup>b)</sup>	21.6	[11]

a) alkali metal carbonate (AMC), alkali earth metal carbonate (AEMC)

b) Passed 100 H 85°C 85% Humidity damp heat test

c) metal acetylacetonate (MAcac)

d) SiN<sub>x</sub> passivated Partial Rear Contact

**Table S2.** Principal input parameters of back contact TiC<sub>x</sub> electron transport solar cell

	p <sup>+</sup>	n	TiC <sub>x</sub> ETL
Thickness (μm)	0.40	180	0.004
E <sub>g</sub> (eV)	1.12	1.12	2.8
N <sub>D</sub> (cm <sup>-3</sup> )	0	1.6 e <sup>15</sup>	1 e <sup>19</sup>
N <sub>A</sub> (cm <sup>-3</sup> )	Gauss diffusion 1 e <sup>20</sup>	0	0
χ (eV)	4.05	4.05	4.04
μ <sub>n</sub> (cm <sup>2</sup> /Vs)	1450	1450	0.5
μ <sub>p</sub> (cm <sup>2</sup> /Vs)	450	450	0.2
N <sub>C</sub> (cm <sup>-3</sup> )	2.8 e <sup>19</sup>	2.8 e <sup>19</sup>	2.8 e <sup>19</sup>
N <sub>V</sub> (cm <sup>-3</sup> )	1.04 e <sup>19</sup>	1.04 e <sup>19</sup>	1.04 e <sup>19</sup>

**Table S3.** Cell performance at 1000H damp heat test.

85°C 85% Humidity test time (H)	V <sub>oc</sub> (mV)	J <sub>sc</sub> (mA/cm <sup>2</sup> )	FF (%)	PCE (%)
40	604	35.75	80.02	17.28
100	600	35.53	81.09	17.31
200	604	35.34	80.82	17.25
300	600	35.57	80.98	17.31
500	604	35.53	81.18	17.42
700	598	35.41	80.49	17.07
800	600	34.83	80.44	16.83
900	600	34.80	79.65	16.65
1000	598	34.76	78.23	16.29

## References

- [1] X. Yang, P. Zheng, Q. Bi and K. Weber, *Solar Energy Materials and Solar Cells*, 2016, **150**, 32-38.
- [2] J. Bullock, Y. Wan, Z. Xu, S. Essig, M. Hettick, H. Wang, W. Ji, M. Boccard, A. Cuevas, C. Ballif and A. Javey, *ACS Energy Letters*, 2018, **3**, 508-513.
- [3] J. Cho, J. Melskens, M. R. Payo, M. Debucquoy, H. S. Radhakrishnan, I. Gordon, J. Szlufcik, W. M. M. Kessels and J. Poortmans, *ACS Applied Energy Materials*, 2019, **2**, 1393-1404.
- [4] Y. Wan, C. Samundsett, J. Bullock, M. Hettick, T. Allen, D. Yan, J. Peng, Y. Wu, J. Cui, A. Javey and A. Cuevas, *Advanced Energy Materials*, 2016, **7**.
- [5] C. Quan, H. Tong, Z. H. Yang, X. X. Ke, M. D. Liao, P. Q. Gao, D. Wang, Z. Z. Yuan, K. M. Chen, J. Yang, X. Y. Zhang, C. H. Shou, B. J. Yan, Y. H. Zeng and J. C. Ye, *Solar Rrl*, 2018, **2**.
- [6] X. Yang, Q. Bi, H. Ali, K. Davis, W. V. Schoenfeld and K. Weber, *Adv Mater*, 2016, **28**, 5891-5897.
- [7] J. Bullock, Y. Wan, M. Hettick, X. Zhaoran, S. P. Phang, D. Yan, H. Wang, W. Ji, C. Samundsett, Z. Hameiri, D. Macdonald, A. Cuevas and A. Javey, *Advanced Energy Materials*, 2019, **9**.
- [8] J. Cho, H. Sivaramakrishnan Radhakrishnan, R. Sharma, M. Recaman Payo, M. Debucquoy, A. van der Heide, I. Gordon, J. Szlufcik and J. Poortmans, *Solar Energy Materials and Solar Cells*, 2020, **206**.
- [9] J. Cho, H. Sivaramakrishnan Radhakrishnan, M. Recaman Payo, M. Debucquoy, A. van der Heide, I. Gordon, J. Szlufcik and J. Poortmans, *ACS Applied Energy Materials*, 2020, **3**, 3826-3834.
- [10] Y. M. Wan, J. Bullock, M. Hettick, Z. R. Xu, C. Samundsett, D. Yan, J. Peng, J. C. Ye, A. Javey and A. Cuevas, *Advanced Energy Materials*, 2018, **8**.
- [11] J. He, W. J. Wang, L. Cai, H. Lin, Z. L. Wang, S. K. Karuturi and P. Q. Gao, *Advanced Functional Materials*, 2020, **30**.